ACS APPLIED MATERIALS & INTERFACES

Research Article

www.acsami.org

Solution-Processed White Organic Light-Emitting Diodes with Enhanced Efficiency by Using Quaternary Ammonium Salt Doped Conjugated Polyelectrolyte

Yuan Tian, Xinjun Xu,* Jinshan Wang, Chuang Yao, and Lidong Li*

State Key Lab for Advanced Metals and Materials, School of Materials Science and Engineering, University of Science and Technology Beijing, Beijing 100083, China

Supporting Information

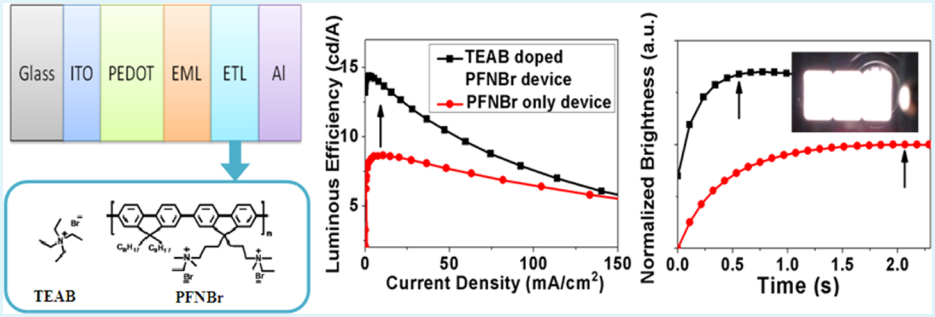

ABSTRACT: Solution-processed white organic light emitting diodes (WOLEDs) with quaternary ammonium salt doped water/alcohol soluble conjugated polyelectrolyte, poly[(9,9-bis(3′-((*N*,*N*-dimethyl)-N-ethylammonium)-propyl)-2,7-fluorene)-*alt*-2,7-(9,9-dioctylfluoren)] dibromide (PFNBr), as electron transport material has been fabricated. Compared with the undoped devices, the performances of such devices with a doped electron transport layer have been dramatically improved to be nearly twice high in luminous efficiency and nearly one-third in response time when the weight ratio of PFNBr to tetraethylammonium bromide (TEAB) was 10:3. Four kinds of quaternary ammonium salts have been investigated to be dopants in the conjugated polyelectrolyte electron transport layer. It has been shown that both the anions and the cations of quaternary ammonium salts can influence the device performance. The dopant who has both a smaller anion and a smaller cation size can exhibit a better device performance. In addition, ultraviolet photoelectron spectroscopy measurement and single-carrier device testing have been employed to investigate the reason why such quaternary ammonium salt dopants can make an obvious improvement in the device performance of WOLEDs. These findings will be beneficial to the progress in design and fabrication of solution-processed WOLEDs suitable for lighting.

KEYWORDS: *conjugated polyelectrolyte, dopant, electron transport material, quaternary ammonium salt, solution-processing, white organic light-emitting diodes*

INTRODUCTION

White organic light-emitting devices (WOLEDs) have attracted much attention in recent years due to their potential applications in next generation flat-panel displays and solid-state lighting. WOLEDs can be fabricated either through a vacuum evaporation method or through a solution-processed one. For the former technique route, multilayer device structure and coevaporation of organic dyes is usually adopted which make the manufacturing process to be complicated. Furthermore, the vacuum evaporation process is time and energy consuming. As a result, WOLEDs fabricated from the latter technique route, that is, the solution processing, have gradually attracted increasing research enthusiasm both in scientific and industrial communities due to their many unique advantages, such as simple device structures, low-cost and facile manufacturing process, compatibility with flexible substrates, and easy processability over large-areas by spin-coating, inkjet printing, or roll-to-roll coating.[1−5] So far, the peak efficiency of small molecules based WOLEDs fabricated by vacuum-deposited technology has already surpassed that of fluorescent lamps.[6] In contrast, the progress of solution-processed WOLEDs is still severely hindered by the relatively low device efficiency arising from the limitation of selecting appropriate carrier transporting layers.[7,8]

In order to achieve high-efficiency WOLEDs, efficient and balanced injection of electrons and holes from electrodes and their transport in the semiconductor layer are necessary. To facilitate the injection and transport of holes, materials such as poly(3,4-ethylene-dioxythiophene):poly(styrene sulfonic acid) (PEDOT:PSS),[9,10] nickel oxide (NiO),[11] vanadium oxides

Received: March 11, 2014
Accepted: April 25, 2014
Published: April 25, 2014

   dx.doi.org/10.1021/am501466y | ACS Appl. Mater. Interfaces 2014, 6, 8631−8638

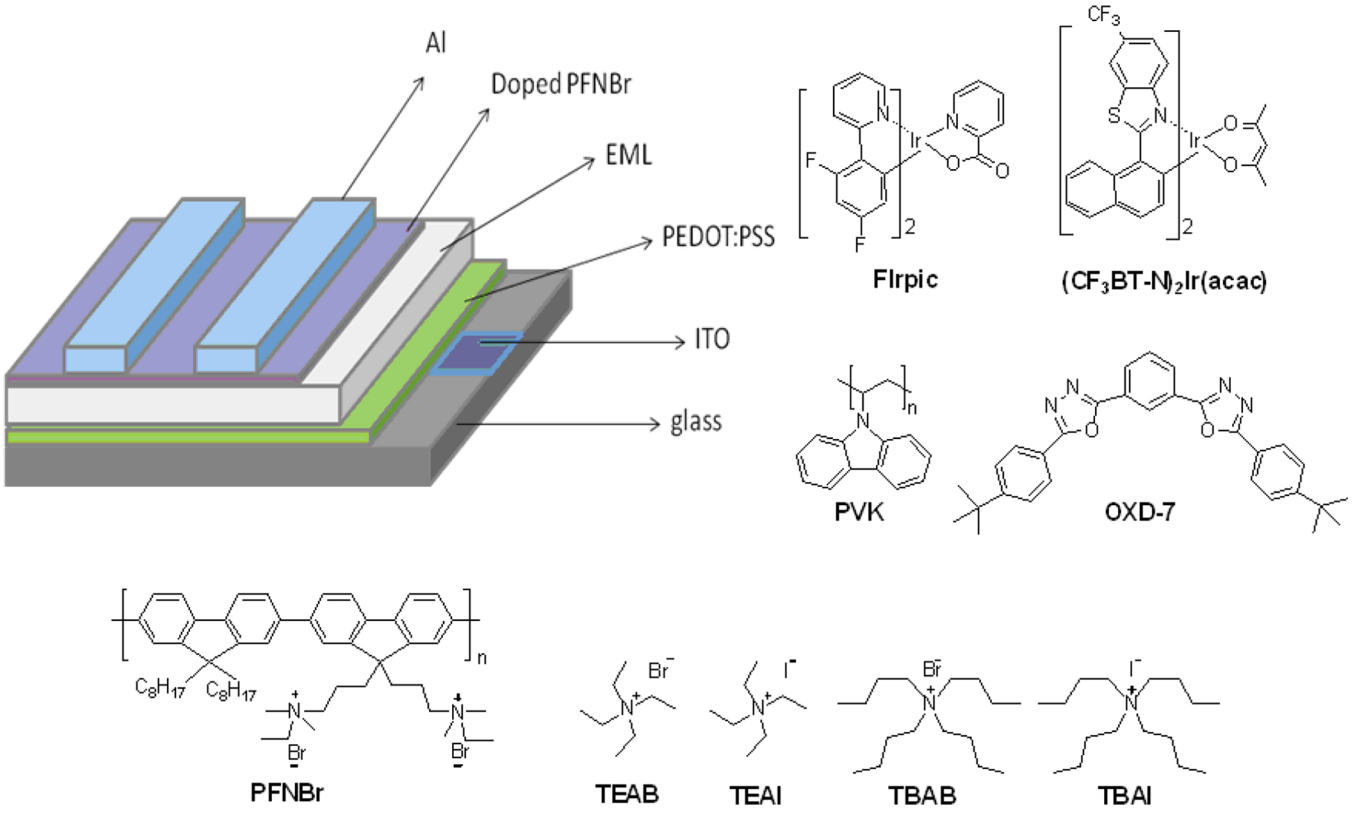

Figure 1. Device structure and chemical structures of relevant materials.

(V_2O_5),[12,13] tungsten oxide (WO_3),[14] molybdenum oxides (MoO_x),[15−17] and cross-linkable triarylamine drivatives have been selected to act as the solution-processed hole injection/transport layer.[18−22] To facilitate electron injection, low work function metals such as Ba and Ca are usually used to achieve high-efficiency devices. Unfortunately, these low work function metals are very sensitive to oxygen and moisture. However, the utilization of quite environment stable metals, such as Al or Ag often shows poor device performances due to a large electron injection barrier existed between the cathode and the emission layer.[23] To overcome such a drawback, many electron-transporting layer (ETL) materials have been developed.[24] In addition, an ultrathin layer of LiF, as well as other alkali salts has been widely used to improve the electron injection in OLEDs.[25,26] Nevertheless, these reported electron-transporting/injecting material layers are usually deposited through a vacuum thermal evaporation method and can hardly be handled by solution-processing. Although some n-type metal oxides such as zinc oxide (ZnO) and titanium oxide (TiO_2) have been developed as electron injection/transport layers through a solution process,[27−29] high-temperature treatment is needed to convert the precursor solution to the desired metal oxide which is incompatible with plastic substrates in roll-to-roll manufacturing.

Recently, several water/alcohol soluble conjugated polymers were developed to be electron transport material for OLEDs, owing to its potential application to replace low work function metals in all solution-processing displays and lighting devices.[30,31] For the convenient and fast fabrication of OLEDs, solution-processed ETL materials attract many researchers' attention. Currently, ETLs made from zwitterionic conjugated polymer,[32] poly(sodium 4-styrenesulfonate) (PSS-Na),[23] and water/alcohol soluble conjugated polymers with polar groups on the side chains, which can form interfacial dipoles between the emitting layer and metal cathode, have been developed.[33−35] In a further step, all-solution processed polymer light-emitting diode displays with solution-deposited Ag cathode and water/alcohol soluble conjugated polymer ETL have been achieved.[31] Because most of the organic semiconductors possess relatively low carrier concentration and mobility, thicker electron-transporting layer often results in increased driving voltage for devices and causes more power consumption. One way to overcome this limitation is to use doped structure to enhance device performance.[36] Although p-doped PEDOT:PSS has been widely used in OLEDs to improve hole injection and transport, the successful development of n-doped materials for efficient electron injection and transport remains very challenging, due to the difficulty of finding suitable hosts and dopants. The unique solubility and excellent electron injection ability of the water/alcohol soluble conjugated polymers offer the possibility to improve electron injection and conduction by doping them with water-soluble salts. Currently, only alkali metal salt Li_2CO_3 has been tested to serve as a dopant in such water/alcohol soluble conjugated polymers which can demonstrate a high device efficiency.[37] However, this kind of device still needs air-unstable metal Ba to act as the cathode.

In this work, we conducted a series of experiments and found that the electron-transporting ability of a water/alcohol soluble conjugated polymer, poly [(9,9-bis(3′-((*N*,*N*-dimethyl)-*N*-ethylammonium)-propyl)-2,7-fluorene)-*alt*-2,7-(9,9-dioctyl-fluorene)] dibromide (PFNBr), can be dramatically improved by doping quaternary ammonium salts. By incorporating this kind of quaternary ammonium salt doped conjugated polymer into solution-processed WOLEDs to act as an electron-transporting layer, significantly enhanced luminous efficiency

and shorter response time can be achieved in such devices compared with the undoped one.

EXPERIMENTAL SECTION

Materials. Poly(*N*-vinylcarbazole) (PVK) and PEDOT:PSS (CLEVIOS PVP Al 4083) were purchased from Sigma-Aldrich and H. C. Starck Clevios GmbH, respectively, and were used as received. 1,3-Bis[(4-*tert*-butylphenyl)-1,3,4-oxadiazolyl]phenylene (OXD-7) was purchased from Wuhan Zossin technology Co., Ltd. PFNBr was purchased from Luminescence Technology Corp. Iridium(III) bis(4,6-difluorophenylpyridinato-N, C2′) picolinate (FIrpic) and bis(2-(naphthalen-1-yl)-6-(trifluoromethyl)benzothiazole)iridium-(acetylacetonate) $(CF_3BT\text{-}N)_2Ir(acac)$ were synthesized according to the literature.[38] Other reagents were obtained from J&K Chemical and used as received. All the solvents were purchased from Beijing Chemical Works and were distilled before use.

Fabrication of WOLEDs. The WOLEDs were fabricated on patterned ITO-coated glass substrates with a sheet resistance of 10 Ω/square purchased from CSG Holding Co., Ltd. The ITO-coated glass substrates were cleaned by detergent, then sequentially ultrasonicated in distilled water, acetone, and alcohol. Subsequently, a layer of 40 nm thick PEDOT:PSS was spin-coated onto the precleaned and ultraviolet-ozone (UVO) treated ITO substrates, then annealed at 120 °C for 30 min in a nitrogen filled glovebox (H_2O < 0.1 ppm, O_2 < 0.1 ppm). After that, a chlorobenzene solution containing the mixture of PVK:OXD-7:FIrpic: $(CF_3BT\text{-}N)_2Ir(acac)$ in a total concentration of 15 mg/mL was spin-coated onto the PEDOT:PSS layer and baked at 120 °C for 10 min to form a 80 nm thick emitting material layer (EML). The ETL material composed of PFNBr and quaternary ammonium salt was dissolved in water/methanol (1:4 v/v) and was spin-coated on the emissive layer by the "on-the-fly-dispensing-spin-coating" method to form a ∼10 nm thickness thin film.[39] Finally, Al (80 nm) was deposited onto the ETL as a cathode by thermal evaporation under a vacuum of 3×10^{-6} Torr.

Measurements. Film thickness was measured by an Ambios Technology XP-2 profilometer. Work function was measured using the ultraviolet photoelectron spectroscopy (UPS) (AXIS Ultra-DLD) with a HeI source ($h\nu$ = 21.22 eV) at a pressure of 3.0×10^{-8} Torr. A bias voltage of −9 V was applied to the sample during the measurements to distinguish between the analyzer and the sample cutoffs. The current density−luminance−voltage (*J*−*L*−*V*), luminous efficiency−current density (*η*−*J*), response time characteristics and lifetimes were measured using a Keithley 2612B source-measurenment unit and a silicon photodiode that is calibrated by a PR-655 SpectraScan spectrophotometer. Electroluminescent (EL) spectra were recorded on a Maya 2000Pro spectrophotometer (Ocean Optics). CIE coordinates were calculated from the EL spectra. The atomic force microscopy (AFM) images were obtained from a Veeco DI Dimension V atomic force microscope operating in the tapping mode.

RESULT AND DISCUSSION

WOLED Properties. We fabricated a series of WOLEDs with quaternary ammonium salt doped PFNBr as the ETL to improve the devices' efficiency. To compare the device performances, WOLEDs with the undoped ETL and without ETL using either Al or Ca cathodes were also fabricated as the control devices. As shown in Figure 1, the device structure used in this study is ITO/PEDOT:PSS/PVK:OXD-7:FIrpic: $(CF_3BT\text{-}N)_2Ir(acac)$ (with a weight ratio of 100:40:10:0.2)/ETL/Al, where PEDOT:PSS is used as the hole injecting layer (HIL), PVK serves as the polymer host, and OXD-7 is doped into the PVK host to improve electron transport in EML. Two emitters including the sky-blue phosphorescent complex FIrpic and the red phosphorescent complex $(CF_3BT\text{-}N)_2Ir(acac)$ are mixed into the PVK host to achieve white-light emission. PFNBr, which is either doped with quaternary ammonium salt or exists as the neat film, is used as the ETL. The chemical structures of the relevant materials are also shown in Figure 1.

We first investigated tetraethylammonium bromide (TEAB) as a dopant in PFNBr with different concentrations to act as ETLs in WOLEDs. The weight ratios of PFNBr to TEAB were 10:1, 10:2, 10:3, and 10:4, respectively. The performances of such WOLEDs are summarized in Table 1.

Table 1. Performances of WOLEDs with and without ETL[a]

ETL and cathode structure	V_{on}[b] (V)	η_{max}[c] (cd A^{-1})	η_{1000}[d] (cd A^{-1})	L_{max}[e] (cd m^{-2})
Al	11.8	0.46		215
Ca/Al	6.0	8.10	8.03	14 185
PFNBr/Al	4.3	8.64	8.61	10 035
PFNBr:TEAB(10:1)/Al	4.6	12.38	12.35	9860
PFNBr:TEAB(10:2)/Al	4.5	12.90	12.80	11 920
PFNBr:TEAB(10:3)/Al	3.9	14.38	13.98	9501
PFNBr:TEAB(10:4)/Al	4.3	12.48	12.16	10 031

[a]The ETL can be either a neat or TEAB doped PFNBr film. [b]Turn-on voltage which is defined as the voltage at a brightness of 1 cd/m^2. [c]Maximum luminous efficiency. [d]Luminous efficiency at a brightness of 1000 cd/m^2. [e]Maximum luminance.

The *J*−*L*−*V* and *η*−*J* characteristics are shown in Figure 2. Obviously, the devices with TEAB doped PFNBr showed excellent device performances. In Figure 2a, we can find that the doped devices showed higher current densities than the undoped one under the same driving voltage. Among them, the doped ETL with a PFNBr:TEAB weight ratio of 10:3 showed the lowest turn-on voltage of 3.9 V. Such a turn-on voltage is much lower than that of devices without using the ETL (see Figure 2b). When the driving voltage further increased, typically larger than 6 V, all the devices with the doped ETL showed a significantly higher brightness than the undoped one. This big difference in brightness can be remained until a high driving voltage (∼13 V) was reached. Meanwhile, compared with devices using undoped ETL, devices with the doped ETL showed obviously increased luminous efficiency. As shown in Figure 2c, the device with a doped ETL (PFNBr:TEAB = 10:3) exhibited a maximum luminous efficiency of 14.38 cd A^{-1}, which was much larger than that of the undoped one. With the doping ratios varying from 10:1 to 10:3, the luminous efficiency was slightly improved. However, further increasing the doping ratio to 10:4, the luminous efficiency began to decline. The device performance parameters are summarized in Table 1; among all the devices, the device with a doping ratio of 10:3 showed the best performance. In contrast, the devices using Al cathode without ETL showed a poor device performance with a very low luminance and luminous efficiency. Replacing the Al cathode with Ca will largely increase the luminous efficiency to be comparable to that of the device with the undoped ETL. However, its value (η_{max} = 8.10 cd A^{-1}) was still much less than that of the devices with the doped ETL. Particularly, the device with the doped PFNBr as ETL showed higher current density than the Ca cathode device when the driving voltage was less than 13 V, which indicated that a better electron injection and transport ability can be achieved in such devices than in Ca cathode based devices.[40,41] This means that by employing a doping strategy in water/alcohol soluble conjugated polymer ETLs, the performance of devices with Al cathode can be significantly improved, which can even be much higher than that of devices using the low-work-function Ca cathode.

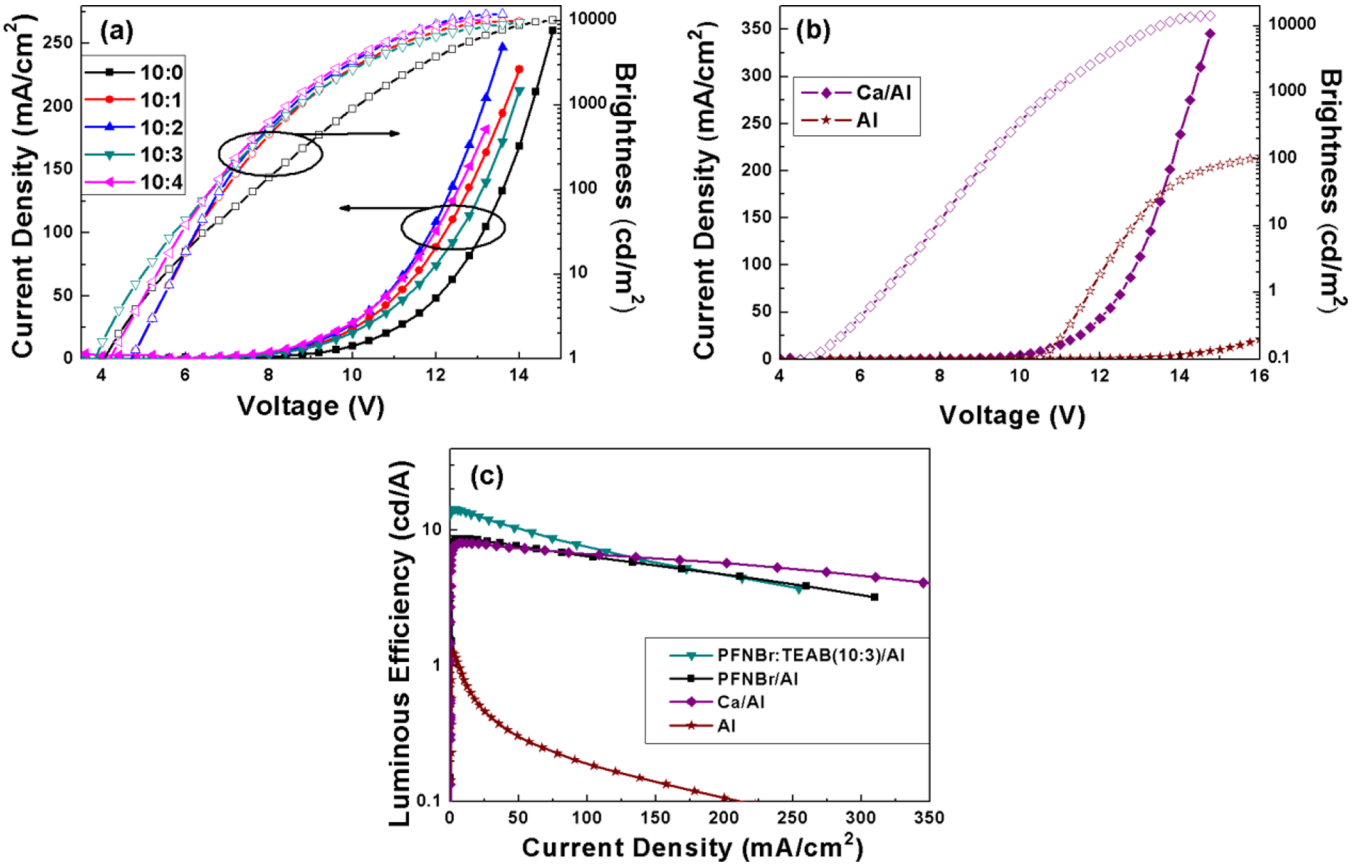

Figure 2. (a) $J-L-V$ characteristics of devices with different doping ratio of TEAB in PFNBr, (b) $J-L-V$ characteristics of devices without the ETL using either a Al or Ca/Al cathode, and (c) $\eta-J$ curves of devices with either doped (PFNBr:TEAB = 10:3) or undoped ETL and without ETL (using either Al or Ca/Al cathode). The filled symbols stand for current density and empty symbols for brightness in parts a and b.

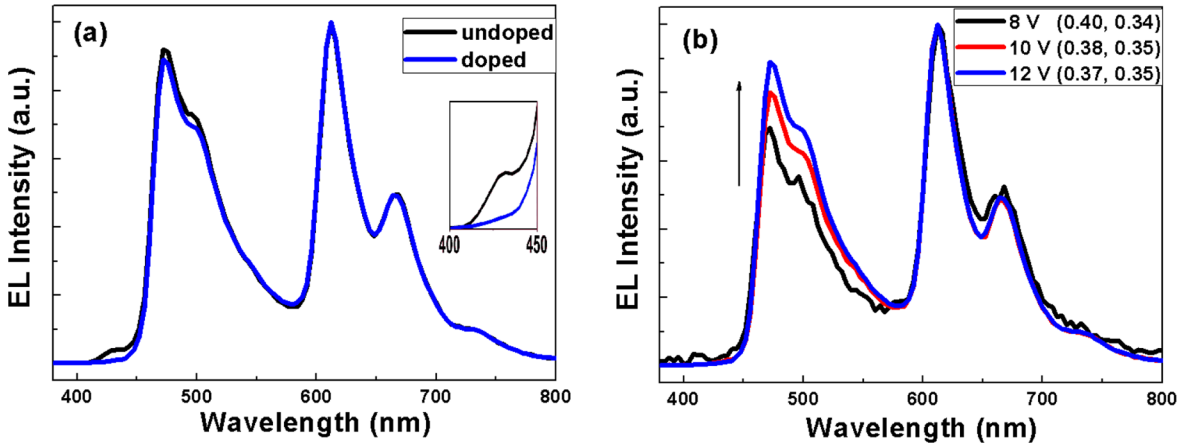

Figure 3. Normalized EL spectra of (a) devices with a doped ETL (PFNBr:TEAB = 10:3) and undoped one at a driving voltage of 12 V (the inset shows the enlargement of curves in a wavelength range of 400–450 nm) and (b) devices with a doped ETL (PFNBr:TEAB = 10:3) at various driving voltages.

The EL spectra of devices with doped and undoped PFNBr as ETLs all exhibited white light emissions and the corresponding Commission Internationale de l'Eclairage (CIE) coordinates were (0.37, 0.35) (@12 V, 6530 cd m^{-2}) and (0.36, 0.35) (@12 V, 3722 cd m^{-2}), respectively. In addition, the EL spectra of the devices with all kinds of doping ratios were almost the same. As shown in Figure 3a, the emission peaks at 472 and 512 nm originated from the emission of FIrpic and the peaks at 612, 668, and 728 nm belonged to the emission of $(CF_3BT\text{-}N)_2Ir(acac)$. The combination emission of these two phosphorescent materials showed a wide spectra ranging from 450 to 800 nm, which is suitable for lighting. It is necessary to note that the device with undoped ETL showed a weak emission peak at 430 nm (Figure 3a). This additional emission peak can be attributed to the emission from PFNBr.[30] This result indicates that some electrons and holes recombined within the PFNBr layer due to its relatively poor electron transport ability, thus leading to the emission of less

efficient blue fluorescence of PFNBr. In contrast, when TEAB was doped into PFNBr, the electron transport ability of ETL was expected to be improved and all the electrons and holes could recombine in the EML. So the emission peak at 430 nm disappeared. The color stability of the device with a doped ETL (PFNBr:TEAB = 10:3) has been shown in Figure 3b. It can be seen that the sky-blue emission peak of FIrpic was gradually enhanced with the increase of driving voltage. Despite such changes in EL spectra, in the luminance range suitable for lighting, the CIE coordinates only varied from (0.40, 0.34) at 8 V (511 cd m^{-2}) to (0.37, 0.35) at 12 V (6530 cd m^{-2}), which all located in the white light region.

Figure 4 shows the normalized brightness−time characteristics at a driving voltage of 10 V for TEAB doped ETL devices

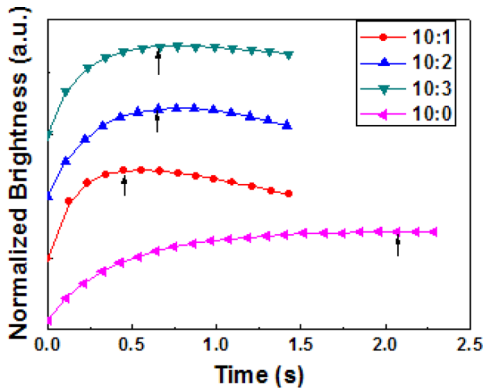

Figure 4. Normalized brightness−time characteristics of devices with TEAB doped ETL using different doping ratios. The ordinate has been shifted for the different curves.

with different doping ratios. We define the time to reach the maximum brightness in devices as the response time. The response time reduced from more than 2 s for the undoped device to 0.45 s when TEAB was doped into ETL in the device with a PFNBr:TEAB ratio of 10:1. When increasing the doping ratio of TEAB, the devices expended a little more time to reach their maximum brightness (0.65 s for the 10:2 device and 0.70 s for the 10:3 device). It is generally considered that the carrier transport ability of PFNBr partially depends on the ion motion,[43] and the ionic charges usually lead to long response times.[32] When TEAB was doped into PFNBr, there must be more ions participated in conducting, which we can regard as less motion distance for every ion. So, it is easy to explain the relatively shorter response times of the doped devices. However, when the doping ratio increased, large aggregates of quaternary ammonium salt may be formed in the ETL, and the interaction between ions may hinder both the ion motion and the formation of dipole layer.[35,43] In other words, it will spend more time for ions to redistribution in the ETL. As a result, we can find the response times became slightly longer for the 10:2 and 10:3 devices compared with the 10:1 device. Additionally, the device lifetime has been measured in order to test the devices' long-term stability (Figure S1, Supporting Information). Because the TEAB doped device can achieve the same brightness under a lower current density, it showed relatively long lifetime compared to the undoped device and Ca/Al device.

In order to explore the influence of doping ions on the device performance, some other quaternary ammonium salts including tetraethylammonium iodide (TEAI), tetrabutylammonium bromide (TBAB), and tetrabutylammonium iodide (TBAI) were also doped into PFNBr as an ETL to fabricate WOLEDs. Each of these three quaternary ammonium salts was doped into PFNBr with a same molar concentration as TEAB in the case of 10:3 weight ratio, so the doping weight ratios of TEAI, TBAB, and TBAI in ETL were 10:3.67, 10:4.60, and 10:5.27, respectively. The performances of such WOLEDs are summarized in Table 2. The corresponding $J-L-V$ and $\eta-J$

Table 2. Performances of WOLEDs using TEAB, TEAI, TBAB, and TBAI Doped PFNBr with the Same Molar Concentration to Act as the ETL

quaternary ammonium salt	V_{on} (V)	η_{max} (cd A^{-1})	η_{1000} (cd A^{-1})	L_{max} (cd m^{-2})
TEAB	3.9	14.38	13.98	9501
TEAI	4.3	10.46	10.39	6749
TBAB	3.8	11.51	11.50	7249
TBAI	3.8	10.46	10.30	6207

curves are shown in Figure 5. As shown in Figure 5a, all the devices exhibited almost the same current densities under the same driving voltage. Additionally, the EL spectra of all the devices were almost the same. However, devices doped with TEAI, TBAB, and TBAI showed a relatively lower maximum brightness and luminous efficiency than the TEAB based device. AFM was used to investigate the microstructure of PFNBr thin films with and without dopants (Figure S2, Supporting Information). The AFM images showed that the undoped PFNBr film exhibited a slightly smooth surface with a root-mean-square roughness (R_q) of 1.08 nm. While, PFNBr films doped with each of the four different quaternary ammonium salts showed similar surface morphology and almost the same surface roughness (about 2.0 nm), which indicated that the microstructure of films may not be the main reason for the EL performance differences among OLEDs with the four quaternary ammonium salt dopants.

It is generally accepted that the enhanced performance in OLED devices after introduction of ETL is correlated with the reduced electron injection barrier and the improved carrier transport ability in devices. Since the action of the polyelectrolyte ETL combines features of OLEDs and light-emitting electrochemical cells (LECs) and involves mixed ionic and electronic conduction,[42] ion movement in the polyelectrolyte ETL should play an important role in charge carrier transport. Because small ions always show a better mobility than big ones,[43,44] movement of $N(C_2H_5)_4^+$ and Br^- in ETL should be easier than $N(C_4H_9)_4^+$ and I^-, respectively. Consequently, polyelectrolyte ETLs with smaller ion dopants show higher charge carrier transport ability than those with larger ion dopants. We think this may be the reason why TEAI, TBAB, and TBAI based devices showed worse performances than TEAB based one.

Characterization of the Doped PFNBr ETL. Clearly, the current density in WOLEDs has increased when doping quaternary ammonium salt into the ETL layer. There are two possible ways to explain this phenomenon. One is that the doping facilitates the charge carrier transport in ETL, and the other is that the electron injection barrier from cathode to ETL has been decreased. In order to test whether the improvement of electron injection is the dominate factor, UPS measurement was performed to determine the work function of the Al cathode coated with either a doped or an undoped PFNBr

dx.doi.org/10.1021/am501466y | ACS Appl. Mater. Interfaces 2014, 6, 8631−8638

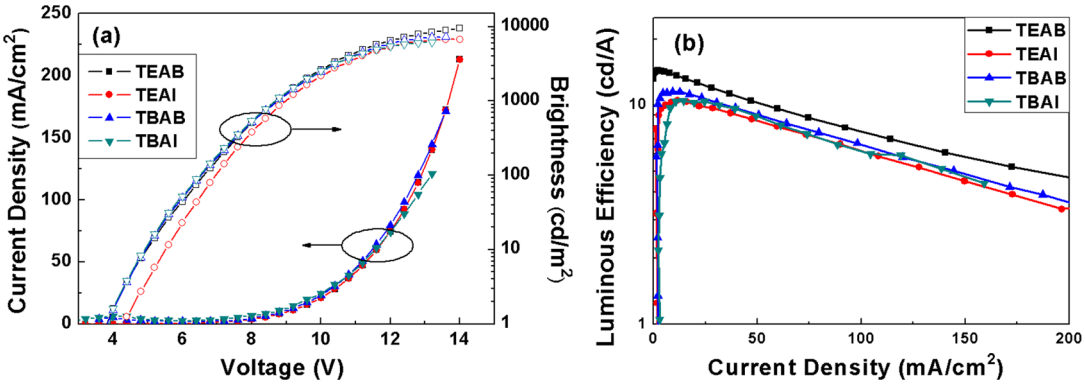

Figure 5. (a) J–L–V and (b) η–J characteristics of WOLEDs with TEAB, TEAI, TBAB, and TBAI doped PFNBr as the ETL. (The filled symbols stand for current density and empty ones stand for brightness.)

layer. As shown in Figure 6, the work function was estimated from the secondary cutoff energy in the UPS spectrum. For the purpose of comparison, the work function of the naked Al with an etching method was also tested and calculated to be 4.22 eV. The work function value of the Al cathode covered either by undoped PFNBr or by TEAB doped one (PFNBr:TEAB = 10:3) is calculated to be 3.02 eV, similarly. Compared with the naked Al, the decrease in work function of ETL covered Al illuminated the improvement of electron injection ability from the cathode to EML. However, the UPS spectra were nearly unchanged for the ETL covered Al regardless of TEAB doping, which indicates that the doped ions of quaternary ammonium salt make no contribution to the lowering of electron injection barrier in our WOLEDs.

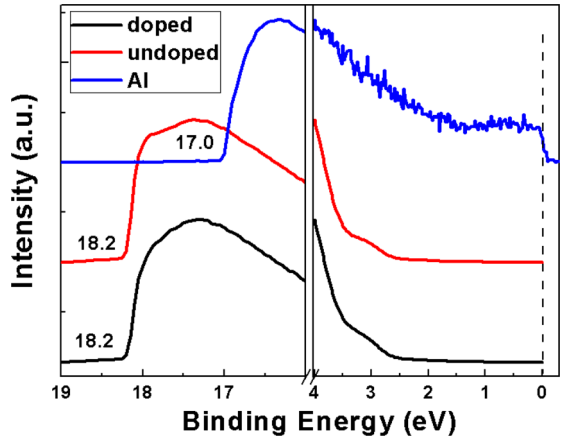

Figure 6. UPS spectra of the naked Al (blue curve) and ETL coated Al comprising the doped PFNBr (PFNBr:TEAB = 10:3, black curve) or the undoped one (red curve). The ordinate has been shifted for the different spectra.

Undoubtedly, the promotion of charge carrier transport ability in ETL by doping quaternary ammonium salt will be the unique explanation of the improvement in devices performance. To verify this hypothesis, electron single-carrier devices with a structure of ITO/Al (80 nm)/PFNBr with or without TEAB doping (85 nm)/Ca (8 nm)/Al (100 nm) and hole single-carrier devices with a structure of ITO/PEDOT:PSS (40 nm)/PVK (12 nm)/ PFNBr with or without TEAB doping (85 nm)/Au (20 nm) were fabricated. As shown in Figure 7a, the electron current densities of the devices with TEAB doped PFNBr were much higher than the undoped one under the same electric field intensity, indicating that the electron-transporting ability of PFNBr was improved by doping. The electron-only device with a doping ratio of 10:3 (PFNBr:TEAB) showed the best improvement in electron transport ability, whose current density was much higher than the undoped device under the same electric field intensity. This result is consistent with the fact that WOLED with the same doping ratio in ETL showed the best luminous efficiency. On the contrary, the hole transport ability dramatically decreased when TEAB was doped into PFNBr (Figure 7b). Among such hole-only devices, the device with a doping ratio of 10:3 showed the minimum current density under the same electric field intensity, which was much less than the undoped device. To sum up, all these results indicate that doping quaternary ammonium salt into PFNBr gives rise to the increase in

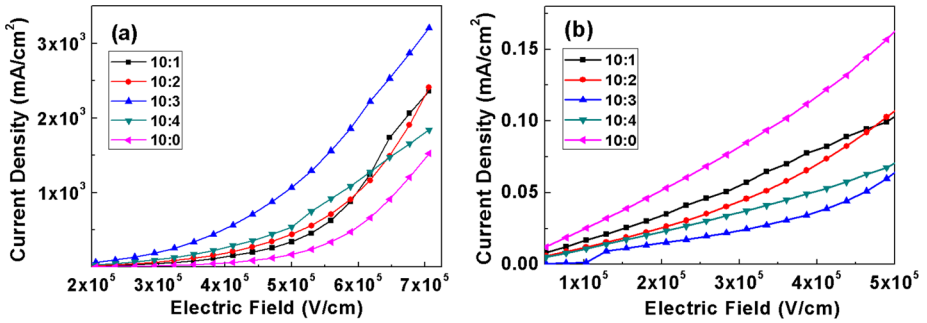

Figure 7. Current density–electric field characteristics of the (a) electron single-carrier and (b) hole single-carrier devices with different PFNBr:TEAB ratios.

dx.doi.org/10.1021/am501466y | ACS Appl. Mater. Interfaces 2014, 6, 8631–8638

electron transport ability and thus the improvement of device performance.

CONCLUSION

Water/alcohol-soluble conjugation polyelectrolyte PFNBr has been doped with quaternary ammonium salts to act as an ETL in WOLEDs. Such a doping strategy can significantly improve the electron transport ability in the ETL, resulting in an enhanced luminous efficiency in WOLEDs compared with those using the undoped ETL. UPS and single-carrier devices measurements can verify that it is the enhanced electron-transporting ability, but not the reduced electron injection barrier, that contributes to the improvement of device performance in WOLEDs. Four types of quaternary ammonium salts including TEAB, TEAI, TBAB, and TBAI have been employed as the dopants in the PFNBr ETL. Results show that the quaternary ammonium salt who has the smallest ion sizes can lead to the best device performance, benefited from its ease of movement in ETL. The influence of doping ratios on the device performance has also been investigated. It is found that there is an optimal doping ratio for the quaternary ammonium salt in polyelectrolyte ETL. WOLED with a doping ratio of 10:3 (PFNBr:TEAB) shows the best performance with a dramatic improvement of maximum luminous efficiency from 8.64 to 14.38 cd A^{-1} and a decrease in response time from more than 2 s to 0.7s compared with that using the undoped ETL. These findings may be of great help for design and preparation of highly efficient electron-transporting material layer, thus being beneficial to the progress of developing solution-processed WOLEDs suitable for lighting.

ASSOCIATED CONTENT

Supporting Information

Device lifetime data and AFM images of the doped/undoped PFNBr films. This material is available free of charge via the Internet at http://pubs.acs.org.

AUTHOR INFORMATION

Corresponding Authors

*Email: lidong@mater.ustb.edu.cn.
*Email: xuxj@mater.ustb.edu.cn.

Notes

The authors declare no competing financial interest.

ACKNOWLEDGMENTS

This work is supported by the National Natural Science Foundation of China (51273020, 51373022), the Fundamental Research Funds for the Central Universities, the Program for Changjiang Scholars and Innovative Research Team in University and the State Key Lab for Advanced Metals and Materials (2012-ZD05), and Research Fund for the Doctoral Program of Higher Education of China (20130006110007).

REFERENCES

(1) D'Andrade, B. W.; Forrest, S. R. White Organic Light-Emitting Devices for Solid-State Lighting. *Adv. Mater.* **2004**, *16*, 1585−1595.
(2) Misra, A.; Kumar, P.; Kamalasanan, M. N.; Chandra, S. White Organic LEDs and Their Recent Advancements. *Semicond. Sci. Technol.* **2006**, *21*, R35−R47.
(3) Wu, H. B.; Ying, L.; Yang, W.; Cao, Y. Progress and Perspective of Polymer White Light-Emitting Devices and Materials. *Chem. Soc. Rev.* **2009**, *38*, 3391−3400.
(4) Kamtekar, K. T.; Monkman, A. P.; Bryce, M. R. Recent Advances in White Organic Light-Emitting Materials and Devices. *Adv. Mater.* **2010**, *22*, 572−582.
(5) Gather, M. C.; Köhnen, A.; Meerholz, K. Ionic Iridium Complex and Conjugated Polymer Used to Solution-Process a Bilayer White Light-Emitting Diode. *Adv. Mater.* **2011**, *23*, 233−248.
(6) Su, S. J.; Gonmori, E.; Sasabe, H.; Kido, J. Highly Efficient Organic Blue-and White-Light-Emitting Devices Having a Carrier- and Exciton-Confining Structure for Reduced Efficiency Roll-Off. *Adv. Mater.* **2008**, *20*, 4189−4194.
(7) Zou, J. H.; Wu, H.; Lam, C. S.; Wang, C. D. Simultaneous Optimization of Charge-Carrier Balance and Luminous Efficacy in Highly Efficient White Polymer Light-Emitting Devices. *Adv. Mater.* **2011**, *23*, 2976−2980.
(8) Zhou, G.; Wong, W.; Suo, S. Recent Progress and Current Challenges in Phosphorescent White Organic Light-Emitting Diodes (WOLEDs). *J. Photochem. Photobiol., C* **2010**, *11*, 133−156.
(9) Voroshazi, E.; Verreet, B.; Buri, A.; Müller, R. Influence of Cathode Oxidation via the Hole Extraction Layer in Polymer: Fullerene Solar Cells. *Org. Electron.* **2011**, *12*, 736−744.
(10) So, F.; Kondakov, D. Degradation Mechanisms in Small-Molecule and Polymer Organic Light-Emitting Diodes. *Adv. Mater.* **2010**, *22*, 3762−3777.
(11) Mashford, B. S.; Nguyen, T.; Wilson, G. J.; Mulvaney, P. All-Inorganic Quantum-Dot Light-Emitting Devices Formed via Low-Cost, Wet-Chemical Processing. *J. Mater. Chem.* **2010**, *20*, 167−172.
(12) Chen, C. P.; Chen, Y. D.; Chuang, S. C. High-Performance and Highly Durable Inverted Organic Photovoltaics Embedding Solution-Processable Vanadium Oxides as an Interfacial Hole-Transporting Layer. *Adv. Mater.* **2011**, *23*, 3859−3863.
(13) Lee, H.; Kwon, Y.; Lee, C. Improved Performances in Organic and Polymer Light-Emitting Diodes Using Solution-Processed Vanadium Pentoxide as a Hole Injection Layer. *J. Soc. Inf. Dispersion* **2012**, *20*, 640−645.
(14) Tan, Z. A.; Li, L.; Cui, C.; Ding, Y. Solution-Processed Tungsten Oxide as an Effective Anode Buffer Layer for High-Performance Polymer Solar Cells. *J. Phys. Chem. C* **2012**, *116*, 18626−18632.
(15) Fu, Q.; Chen, J.; Shi, C.; Ma, D. Room-Temperature Sol-Gel Derived Molybdenum Oxide Thin Films for Efficient and Stable Solution-Processed Organic Light-Emitting Diodes. *ACS Appl. Mater. Interfaces* **2013**, *5*, 6024−6029.
(16) Matsushima, T.; Kinoshita, Y.; Murata, H. Formation of Ohmic Hole Injection by Inserting an Ultrathin Layer of Molybdenum Trioxide between Indium Tin Oxide and Organic Hole-Transporting Layers. *Appl. Phys. Lett.* **2007**, *91*, 253504.
(17) Zilberberg, K.; Meyer, J.; Riedl, T. Solution Processed Metal-Oxides for Organic Electronic Devices. *J. Mater. Chem. C* **2013**, *1*, 4796−4815.
(18) Zuniga, C. A.; Barlow, S.; Marder, S. R. Approaches to Solution-Processed Multilayer Organic Light-Emitting Diodes Based on Cross-Linking. *Chem. Mater.* **2010**, *23*, 658−681.
(19) Huang, F.; Cheng, Y.; Zhang, Y.; Liu, M. S.; Jen, A. K. Y. Crosslinkable Hole-Transporting Materials for Solution Processed Polymer Light-Emitting Diodes. *J. Mater. Chem.* **2008**, *18*, 4495−4509.
(20) Yan, H.; Scott, B. J.; Huang, Q.; Marks, T. J. Enhanced Polymer Light-Emitting Diode Performance Using a Crosslinked-Network Electron-Blocking Interlayer. *Adv. Mater.* **2004**, *16*, 1948−1953.
(21) Sun, Y.; Gong, X.; Hsu, B. B. Y.; Yip, H.; Jen, A. K. Y.; Heeger, A. J. Solution-Processed Cross-Linkable Hole Selective Layer for Polymer Solar Cells in the Inverted Structure. *Appl. Phys. Lett.* **2010**, *97*, 193310.
(22) Lin, Y.; Lin, C.; Chen, Y.; Chen, H.; Fang, F.; Hung, W.; Kwong, R. C. Hole Mobilities of Thermally Polymerized Triaryldiamine Derivatives and their Application as Hole-Transport Materials in Organic Light-Emitting Diodes (OLEDs). *Org. Electron.* **2009**, *10*, 181−188.
(23) Lim, G. E.; Ha, Y. E.; Jo, M. Y.; Park, J.; Kang, Y. C.; Kim, J. H. Nonconjugated Anionic Polyelectrolyte as an Interfacial Layer for the

Organic Optoelectronic Devices. *ACS Appl. Mater. Interfaces* **2013**, *5*, 6508−6513.
(24) Hughes, G.; Bryce, M. R. Electron-Transporting Materials for Organic Electroluminescent and Electrophosphorescent Devices. *J. Mater. Chem.* **2005**, *15*, 94−107.
(25) Hung, L. S.; Tang, C. W.; Mason, M. G. Enhanced Electron Injection in Organic Electroluminescence Devices Using an Al/LiF Electrode. *Appl. Phys. Lett.* **1997**, *70*, 152−154.
(26) Li, Y.; Zhang, D.; Duan, L.; Zhang, R.; Wang, L.; Qiu, Y. Elucidation of The Electron Injection Mechanism of Evaporated Cesium Carbonate Cathode Interlayer for Organic Light-Emitting Diodes. *Appl. Phys. Lett.* **2007**, *90*, 012119.
(27) Sun, Y. M.; Seo, J. H.; Takacs, C. J.; Seifter, J.; Heeger, A. J. Inverted Polymer Solar Cells Integrated with a Low-Temperature-Annealed Sol-Gel-Derived ZnO Film as an Electron Transport Layer. *Adv. Mater.* **2011**, *23*, 1679−1683.
(28) Lu, L. P.; Kabra, D.; Friend, R. H. Barium Hydroxide as an Interlayer between Zinc Oxide and a Luminescent Conjugated Polymer for Light-Emitting Diodes. *Adv. Funct. Mater.* **2012**, *22*, 4165−4171.
(29) Bolink, H. J.; Coronado, E.; Repetto, D.; Sessolo, M.; Barea, E. M. Inverted Solution Processable OLEDs Using a Metal Oxide as an Electron Injection Contact. *Adv. Funct. Mater.* **2008**, *18*, 145−150.
(30) Wu, H.; Huang, F.; Mo, Y.; Yang, W.; Wang, D.; Peng, J. Efficient Electron Injection from a Bilayer Cathode Consisting of Aluminum and Alcohol-/Water-Soluble Conjugated Polymers. *Adv. Mater.* **2004**, *16*, 1826−1830.
(31) Zheng, H.; Zheng, Y.; Liu, N.; Ai, N.; Wang, Q. All-Solution Processed Polymer Light-Emitting Diode Displays. *Nat. Commun.* **2013**, *4*, 1971.
(32) Fang, J. F.; Wallikewitz, B. H.; Gao, F.; Tu, G. L.; Muller, C. Conjugated Zwitterionic Polyelectrolyte as the Charge Injection Layer for High-Performance Polymer Light-Emitting Diodes. *J. Am. Chem. Soc.* **2011**, *133*, 683−685.
(33) Wu, H. B.; Huang, F.; Mo, Y. Q.; Yang, W.; Peng, J. B.; Cao, Y. Efficient Electron Injection from Bilayer Cathode Consisting of Aluminum and Alcohol/Water-Soluble Conjugated Polymers. *J. Soc. Inf. Dispersion* **2005**, *13*, 123−130.
(34) Yang, R. Q.; Wu, H. B.; Cao, Y.; Bazan, G. C. Control of Cationic Conjugated Polymer Performance in Light Emitting Diodes by Choice of Counterion. *J. Am. Chem. Soc.* **2006**, *128*, 14422−14423.
(35) Huang, F.; Niu, Y. H.; Zhang, Y.; Ka, J. W.; Liu, M. S.; Jen, A. A Conjugated, Neutral Surfactant as Electron-Injection Material for High-Efficiency Polymer Light-Emitting Diodes. *Adv. Mater.* **2007**, *19*, 2010−2014.
(36) Walzer, K.; Maennig, B.; Pfeiffer, M.; Leo, K. Highly Efficient Organic Devices Based on Electrically Doped Transport Layers. *Chem. Rev.* **2007**, *107*, 1233−1271.
(37) Huang, F.; Shih, P.; Shu, C.; Chi, Y.; Jen, A. K. Y. Highly Efficient Polymer White-Light-Emitting Diodes Based on Lithium Salts Doped Electron Transporting Layer. *Adv. Mater.* **2009**, *21*, 361−365.
(38) Lamansky, S.; Thompson, M. E.; Djurovich, P.; Murphy, D.; Abdel-Razzaq, F. Synthesis and Characterization of Phosphorescent Cyclometalated Iridium Complexes. *Inorg. Chem.* **2001**, *40*, 1704−1711.
(39) Zhang, F.; Di, C.; Berdunov, N.; Hu, Y.; Hu, Y.; Gao, X.; Meng, Q.; Sirringhaus, H.; Zhu, D. Ultrathin Film Organic Transistors: Precise Control of Semiconductor Thickness via Spin-Coating. *Adv. Mater.* **2013**, *25*, 1401−1407.
(40) Zhang, Y.; Huang, F.; Chi, Y.; Jen, A. K. Y. Highly Efficient White Polymer Light-Emitting Diodes Based on Nanometer-Scale Control of the Electron Injection Layer Morphology through Solvent Processing. *Adv. Mater.* **2008**, *20*, 1565−1570.
(41) An, D.; Zou, J.; Wu, H.; Peng, J.; Yang, W.; Cao, Y. White Emission Polymer Light-Emitting Devices with Efficient Electron Injection from Alcohol/Water-Soluble Polymer/Al Bilayer Cathode. *Org. Electron.* **2009**, *10*, 299−304.
(42) Hoven, C.; Yang, R.; Garcia, A.; Heeger, A. J.; Nguyen, T. Q.; Bazan, G. C. Ion Motion in Conjugated Polyelectrolyte Electron Transporting Layers. *J. Am. Chem. Soc.* **2007**, *129*, 10976−10977.
(43) Hoven, C. V.; Garcia, A.; Bazan, G. C.; Nguyen, T. Recent Applications of Conjugated Polyelectrolytes in Optoelectronic Devices. *Adv. Mater.* **2008**, *20*, 3793−3810.
(44) Cimrová, V.; Schmidt, W.; Rulkens, R.; Schulze, M.; Meyer, W.; Neher, D. Efficient Blue Light Emitting Devices Based on Tigid-Rod Polyelectrolytes. *Adv. Mater.* **1996**, *8*, 585−588.